AIAA Journal
Vol. 46, No. 2, February 2008

Deformation and Flexibility Equations for Curved, End-Loaded, Planar Elastica

R. David Hampton*
U. S. Military Academy, West Point, New York 10996
Michael J. Leamy†
MITRE Corporation, McLean, Virginia 22102
Paul J. Bryant‡
United Defense, Louisville, Kentucky 40214
and
Naveed Quraishi§
NASA Johnson Space Center, Houston, Texas 77058

DOI: 10.2514/1.18467

The International Space Station relies on the active rack isolation system as the central component of an integrated, station-wide strategy to isolate microgravity space-science experiments. The isolation system uses electromechanical actuators to isolate an international standard payload rack from disturbances due to the motion of the station. Disturbances to microgravity experiments on isolated racks are transmitted primarily via the isolation-system power and vacuum umbilicals. Experimental tests indicate that these umbilicals resonate at frequencies outside the controller's bandwidth, at levels of potential concern for certain microgravity experiments. Reduction in the umbilical resonant frequencies could help to address this issue. Toward that end, this work documents the development and verification of static equations for the in-plane deflections and flexibilities of an idealized umbilical (thin, flexible, elastic, inextensible, prismatic cantilever beam) under endpoint, in-plane loading (inclined force and moment). Gravity is neglected due to the on-orbit application. The analysis assumes that the umbilical experiences large static deflections from a reference curve describing its relaxed configuration, for which the slope follows a quadratic function of arc length. The treatment is applicable to the power and vacuum umbilicals, under the indicated assumptions.

Nomenclature

a_i = arbitrary constant, $i = 0, 1, 2$
C = umbilical terminus
C_1 = integration constant
c_ξ = cosine of umbilical angle ξ at arbitrary point R on umbilical
E = Young's modulus of elasticity
EI = flexural rigidity
F = arbitrary function
f, g = arbitrary functions
I = area moment of inertia with respect to umbilical neutral axis
L = umbilical length
M = internal moment
M_x = terminally applied moment about x axis
O = umbilical origin
P_z = terminally applied force, negative z direction
Q_y = terminally applied force, y direction
Q_z = terminally applied force, z direction
R = arbitrary point along umbilical
s = distance along umbilical from cantilevered end, point O
s_ξ = sine of umbilical angle ξ at arbitrary point R on umbilical
y = position coordinate for arbitrary point R on umbilical
y_c = position coordinate for umbilical terminus, point C
z = position coordinate for arbitrary point R on umbilical
z_c = position coordinate for umbilical terminus, point C
α_i = convenience variable
β_i = flexibility integral
η = square of shape kernel
θ = shape kernel
κ^i = umbilical initial (unloaded) curvature
κ^i_c = umbilical initial curvature at terminus C
λ = load-magnification factor
ν = Poisson's ratio
ξ = final (loaded-umbilical) angle of tangent to umbilical at arbitrary point R
ξ_c = final (loaded-umbilical) angle of tangent to umbilical at terminal point C
ρ = circular-arc test-umbilical radius of curvature, relaxed configuration
ς = initial (unloaded-umbilical) angle of tangent to umbilical at arbitrary point R
ς_c = initial (unloaded-umbilical) angle of tangent to umbilical at terminal point C

Presented as Paper 6179 at the 40th and 41st Aerospace Sciences Meeting & Exhibit (AIAA-2002-1132 for theory, AIAA-2003-6179 for verification), Reno, NV, 6–9 January 2003; received 27 June 2005; revision received 23 June 2007; accepted for publication 1 July 2007.

*Professor, Department of Civil and Mechanical Engineering. Member AIAA.
†Research Scientist, Emerging Technology Office. Member AIAA.
‡Senior Engineer, Engineering Department.
§Manager, Active Rack Isolation System International Space Station Characterization Experiment, International Space Station Payloads Office.

Introduction

THE active rack isolation system (ARIS) serves as the central component of an integrated, station-wide strategy to isolate microgravity space-science experiments on the International Space Station (ISS). ARIS uses eight electromechanical actuators to isolate an international standard payload rack (ISPR) from disturbances due to the motion of the ISS; five ARIS racks comprise the complement for the ISS. Disturbances to microgravity experiments on ARIS-isolated racks are transmitted primarily via the (nominally 13) ARIS umbilicals, which provide power, data, vacuum, cooling, and other miscellaneous services to the experiments. The two power umbilicals and, to a lesser extent, the vacuum umbilical, serve as the primary transmission paths for acceleration disturbances. Experimental tests conducted by the ARIS team [1] (December 1998) indicate that looped power umbilicals resonate at about 10 Hz; unlooped power umbilicals resonate at about 4 Hz. In either case, the ARIS controller's limited bandwidth (about 2 Hz) admits only limited active isolation at these frequencies. Reduction in the umbilical resonant frequencies could help to address this problem.

Analytical studies of the static nonlinear bending and deflection of a thin, flexible, plane-symmetric ("two-dimensional") beam, incorporating Kirchhoff assumptions, have been conducted for a variety of loading conditions. Typically, the beam has been assumed to be inextensible, linearly elastic, fixed-end, and cantilevered (originally horizontal), with transverse-shear and cross-sectional warping neglected. Applied loading conditions that have been treated in the literature for such beams include concentrated terminal transverse (vertical) loading [2–6], uniformly distributed vertical loading [2,7–9], uniformly distributed normal loading [10], concentrated terminal inclined loading [11,12], multiple concentrated vertical loads [13], concentrated terminal vertical and moment loading [13], and heavy, rigid, end-attachment loading [14]. Exact explicit solutions have been found for the static planar deflections of slender two-dimensional beams under certain simple loading conditions; typically, these solutions involve complete and incomplete elliptic integrals (for example, [2,4–6,13–15]). Manuel and Lee [16] provide a set of implicit nonlinear deflection equations for the static case of a weightless flexible two-dimensional beam with arbitrary, discrete, in-plane loads and boundary conditions. References [17–26] provide derivations and numerical examples. For helpful literature reviews, see [17,27–29].

Recent efforts have included treatments of the full dynamics of space beams undergoing large deflections and rotations [30,31]. Geometrically exact dynamic equations of motion exist for such beams, to include inertial, transverse-shear, and cross-sectional warping effects; see especially [32–36].

In regard to the special case of general terminal in-plane loading, that is, for an end load comprising both inclined-force and moment loads, the in-plane flexibility (or stiffness) equations are of particular interest toward umbilical design for microgravity-isolation purposes. In particular, such equations offer possibilities for optimizing umbilical flexibilities and low-end resonant frequencies in microgravity applications. Because it was the intent of the authors to determine exact analytical expressions for static umbilical flexibilities, they restricted their efforts to a two-dimensional beam (elastica) at equilibrium under static terminal end loading. In particular, inertial, transverse-shear, and cross-sectional warping effects were not included for the present analysis. These approximations were reasonable for a typical ARIS umbilical in static equilibrium, and made the problem analytically tractable.

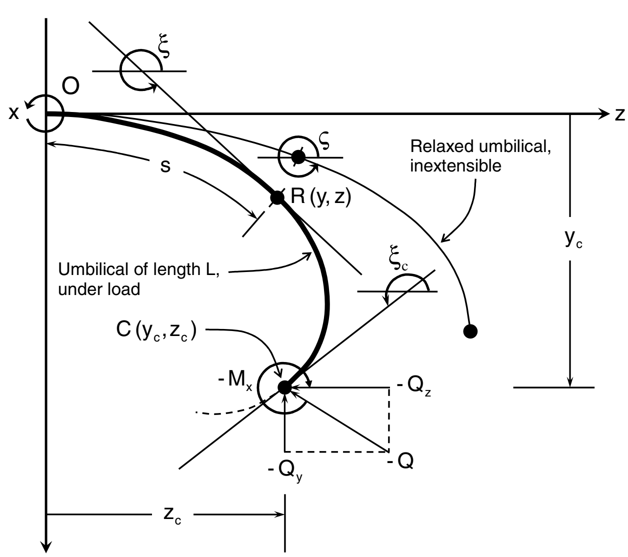

Fig. 1 Flexible umbilical under static end loading.

In-plane deflection and flexibility equations for a two-dimensional elastica that was linear in its relaxed position were reported previously [37]. As a generalization of that effort, this work documents the development and verification of equations, under conditions of static equilibrium, for the in-plane deflections and flexibilities of an initially curved, idealized two-dimensional umbilical subject to terminal in-plane loading (inclined-force and moment). The effect of gravity is neglected, an appropriate approximation for an on-orbit application. The deflection and flexibility analyses are applicable to a cantilevered umbilical which, when unloaded, is curved with a monotonically changing slope that is a quadratic function of arc length. The umbilical possesses uniform cross section, and undergoes large deflections with no plastic deformation, such that the slope of the loaded umbilical also changes monotonically (a realistic assumption for ARIS umbilicals).

Problem Statement

Consider an idealized, curved umbilical of length L with endpoints O and C and arbitrary intermediate point R (Fig. 1). The umbilical is idealized in the same sense as in the preceding section: it is thin, flexible, inextensible, prismatic, linearly elastic, fixed-end, and cantilevered, with equal tensile and compressive moduli of elasticity E. Let R be located at distance s along the umbilical, measured from the cantilevered end (point O), with coordinates (y, z); the coordinates of point C are (y_c, z_c). The coordinates have been chosen to be consistent with the coordinate system in use for the existing analyses of ARIS, for dynamic-modeling and controller-design purposes; point O, then, is the umbilical point of attachment to the ISS, and point C is the point of attachment to the ISPR. Initially, when the umbilical is relaxed (unloaded), let it be described by an "initial" curvature of $\kappa^i(s)$ that varies quadratically with arc length s. If ς is the angle, at R, of the tangent to the umbilical, then this initial curvature is $\mathrm{d}\varsigma/\mathrm{d}s$. (Note that, as indicated in Fig. 1, all angles in this paper are measured in a counterclockwise direction from the $+z$ axis.) When the umbilical is under end load, let the angle of the tangent at R be ξ, and let ξ_c represent the endpoint angle at C. Assume that ξ varies monotonically with distance s (as is the case with the ARIS umbilicals), and that the flexural rigidity EI is known. It should be evident from physical considerations that the assumption of monotonicity for ξ cannot be made for large vibrations about this equilibrium position. However, for small enough vibrations, the assumption will be hold. For simplicity, the present work considers only the case of a beam at equilibrium, under static loading.

This research accomplishes the following fundamental tasks for the previously described beam: 1) to derive geometric equations for the umbilical length, coordinates at arbitrary point R, and terminal coordinates (at C), and 2) to use these equations to derive useful equations for the nine in-plane umbilical flexibilities. These 14 equations will be expressed in terms of the final slope function $\xi(s)$, the terminal angle ξ_c, the initial (unloaded) curvature function $\kappa^i(s)$, the unloaded terminal curvature κ^i_c, and arbitrary in-plane loads at C. The (static) loads are as follows: forces Q_y and Q_z (assumed to be positive in the positive y and z directions, respectively), and moment M_x (assumed to be positive in the counterclockwise direction, about the positive x axis).

Equations of Umbilical Geometry

At point R, the moment equation is

$$-M = M_x + Q_z(y_c - y) - Q_y(z_c - z) = EI\left(\frac{\mathrm{d}\xi}{\mathrm{d}s} - \frac{\mathrm{d}\varsigma}{\mathrm{d}s}\right) \qquad (1)$$

Observe that Eq. (1) is an ordinary differential equation in s, with three dependent variables: y, z, and ξ. However (as is evident from physical considerations), y, z, and ξ are not independent. For the range of arc length $0 \le s \le L$, confine the reference configuration ς to the set of monotonically changing curves describable by a quadratic polynomial function of s:

$$\varsigma = a_2 s^2 + a_1 s + a_0 \tag{2}$$

Then Eq. (1) can be reexpressed in terms of a single dependent variable, angle ξ, by differentiating with respect to s, and incorporating the two holonomic constraints via the following substitutions:

$$\frac{\mathrm{d}y}{\mathrm{d}s} = -\sin\xi \tag{3}$$

and

$$\frac{\mathrm{d}z}{\mathrm{d}s} = \cos\xi \tag{4}$$

The result, using the shorthand notations $s_\xi = \sin\xi$ and $c_\xi = \cos\xi$, is

$$\frac{\mathrm{d}^2\xi}{\mathrm{d}s^2} = 2a_2 + \frac{1}{EI}(Q_z s_\xi + Q_y c_\xi) \tag{5}$$

Equation (5) is a second-order, nonlinear, ordinary differential equation, with single dependent variable ξ and independent variable s. Its integration will yield an expression for $\mathrm{d}\varsigma/\mathrm{d}s$, which can be used in turn to determine equations for the umbilical geometry. Proceeding accordingly, one obtains

$$\frac{1}{2}\left(\frac{\mathrm{d}\xi}{\mathrm{d}s}\right)^2 = 2a_2\xi + \frac{1}{EI}(Q_y s_\xi - Q_z c_\xi) + C_1 \tag{6}$$

where C_1 is an integration constant that can be evaluated with the help of Eq. (1). In particular, at point C, Eq. (1) becomes

$$M_x = EI\left(\frac{\mathrm{d}\xi}{\mathrm{d}s} - \frac{\mathrm{d}\varsigma}{\mathrm{d}s}\right)\bigg|_{R\to C} \tag{7}$$

leading to

$$\frac{\mathrm{d}\xi}{\mathrm{d}s}\bigg|_{R\to C} = \frac{M_x}{EI} + \frac{\mathrm{d}\varsigma}{\mathrm{d}s}\bigg|_{R\to C} = \frac{M_x}{EI} + \kappa_c^i \tag{8}$$

Upon applying this boundary condition to Eq. (6) and rearranging, one has

$$C_1 = \frac{1}{2}\left[\left(\frac{M_x}{EI} + \kappa_c^i\right)^2 - 4a_2\xi_c\right] - \frac{1}{EI}(Q_y s_{\xi_c} - Q_z c_{\xi_c}) \tag{9}$$

such that Eq. (6) can now be solved for $\mathrm{d}\xi/\mathrm{d}s$:

$$\frac{\mathrm{d}\xi}{\mathrm{d}s} = \pm\left\{\frac{2}{EI}[Q_y(s_\xi - s_{\xi_c}) - Q_z(c_\xi - c_{\xi_c})] + \left(\frac{M_x}{EI} + \kappa_c^i\right)^2 + 4a_2(\xi - \xi_c)\right\}^{1/2} = \pm\eta^{1/2} \tag{10}$$

where the radicand η is nonnegative:

$$\eta \equiv \frac{2Q_y}{EI}(s_\xi - s_{\xi_c}) - \frac{2Q_z}{EI}(c_\xi - c_{\xi_c}) + \left(\frac{M_x}{EI} + \kappa_c^i\right)^2 + 4a_2(\xi - \xi_c) \ge 0 \tag{11}$$

Note that

$$\frac{d\xi}{\mathrm{d}s} \le 0 \Leftrightarrow \frac{d\xi}{\mathrm{d}s} = -\eta^{1/2} \tag{12}$$

and that

$$\frac{\mathrm{d}\xi}{\mathrm{d}s} \ge 0 \Leftrightarrow \frac{\mathrm{d}\xi}{\mathrm{d}s} = \eta^{1/2} \tag{13}$$

From Eq. (10),

$$\mathrm{d}\,s = \frac{\mathrm{d}\xi}{\pm\sqrt{\eta}} \tag{14}$$

Define, for convenience, a "shape kernel,"

$$\theta = \pm\sqrt{\eta} \tag{15}$$

where the sign is chosen from the physical considerations of Eqs. (12) and (13), such that

$$\mathrm{d}\,s = \theta^{-1}\,\mathrm{d}\xi \tag{16}$$

(In particular, the upper sign applies when $\mathrm{d}\xi/\mathrm{d}s \ge 0$; the lower, when $\mathrm{d}\xi/\mathrm{d}s \le 0$. This convention will be used throughout the remainder of the paper.) Eq. (16) can be integrated to yield an expression for the umbilical length:

$$L = \int_0^L \mathrm{d}s = -\int_{\xi_c}^{2\pi} \theta^{-1}\,\mathrm{d}\xi \tag{17}$$

From Eq. (3),

$$\mathrm{d}\,y = -s_\xi\,\mathrm{d}s = -\theta^{-1} s_\xi\,\mathrm{d}\xi \tag{18}$$

such that

$$y = \int_\xi^{2\pi} \theta^{-1} s_\xi\,\mathrm{d}\xi\left(= \pm\int_\xi^{2\pi} \eta^{-1/2} s_\xi\,\mathrm{d}\xi\right) \tag{19}$$

and

$$y_c = \int_{\xi_c}^{2\pi} \theta^{-1} s_\xi\,\mathrm{d}\xi\left(= \pm\int_{\xi_c}^{2\pi} \eta^{-1/2} s_\xi\,\mathrm{d}\xi\right) \tag{20}$$

Likewise, Eq. (4) yields

$$z = -\int_\xi^{2\pi} \theta^{-1} c_\xi\,\mathrm{d}\xi\left(= \mp\int_\xi^{2\pi} \eta^{-1/2} c_\xi\,\mathrm{d}\xi\right) \tag{21}$$

and

$$z_c = -\int_{\xi_c}^{2\pi} \theta^{-1} c_\xi\,\mathrm{d}\xi\left(= \mp\int_{\xi_c}^{2\pi} \eta^{-1/2} c_\xi\,\mathrm{d}\xi\right) \tag{22}$$

Together, Eqs. (17) and (19–22) describe the umbilical geometry as unique functions of the terminal angle ξ_c, the terminal loads Q_y, Q_z, and M_x, and the shape kernel θ.

As a check of the aforementioned, in the special case of a horizontal cantilever beam, it can be shown that the preceding geometric equations reduce to known results, for certain simple end loads. In particular, with a vertical (i.e., transverse) point load at the free end, the equations reduce to the solution previously reported in [13], page 41. With a horizontal column load (once buckling occurs), the equations also reduce to known results ([13], page 42).

Equations of Umbilical Flexibility

Nature of Dependencies on Flexural Rigidity

It will now be shown that, for constant values of L, ξ_c, y_c, and z_c, that is, umbilical length and terminal geometry, the following expressions are also constants: Q_y/EI, Q_z/EI, and M_x/EI. This will have important implications for umbilical shapes and flexibilities.

For convenience, define the following variables

$$\alpha_1 = \frac{Q_y}{EI} \tag{23}$$

$$\alpha_2 = \frac{Q_z}{EI} \tag{24}$$

$$\alpha_3 = \frac{M_x}{EI} + \kappa_c^i \tag{25}$$

$$\alpha_4 = \alpha_1 c_{\xi_c} + \alpha_2 s_{\xi_c} \tag{26}$$

and

$$\alpha_5 = 4a_2(\xi - \xi_c) \tag{27}$$

In the case of multiple umbilicals, let an additional subscript indicate the umbilical number, e.g., $\alpha_{ij}, \theta_j, y_j, y_{cj}, \xi_{cj}$. These symbols will be used in the subsequent development.

Consider now two umbilicals of uniform cross section, with identical lengths and terminal geometries, but different flexural rigidities EI and thus different (nonzero) terminal loads. In particular,

$$L_1 = L_2 = L > 0 \tag{28}$$

$$y_{c1} = y_{c2} = y_c \tag{29}$$

$$z_{c1} = z_{c2} = z_c \tag{30}$$

and

$$\xi_{c1} = \xi_{c2} = \xi_c \tag{31}$$

but

$$(EI)_1 \neq (EI)_2 \tag{32}$$

Then

$$L_1 = -\int_{\xi_c}^{2\pi} \theta_1^{-1}\, \mathrm{d}\xi = -\int_{\xi_c}^{2\pi} \theta_2^{-1}\, \mathrm{d}\xi = L_2 \tag{33}$$

$$y_{c1} = \int_{\xi_c}^{2\pi} \theta_1^{-1} s_\xi \Delta \mathrm{d}\xi = \int_{\xi_c}^{2\pi} \theta_2^{-1} s_\xi\, \mathrm{d}\xi = y_{c2} \tag{34}$$

and

$$z_{c1} = -\int_{\xi_c}^{2\pi} \theta_1^{-1} c_\xi\, \mathrm{d}\xi = -\int_{\xi_c}^{2\pi} \theta_2^{-1} c_\xi\, \mathrm{d}\xi = z_{c2} \tag{35}$$

where

$$\theta_j(\xi_j) = \pm[2\alpha_{1j}(s_\xi - s_{\xi_c}) - 2\alpha_{2j}(c_\xi - c_{\xi_c}) + (\alpha_{3j}^2 + \alpha_{5j})]^{1/2} \tag{36}$$

From orthogonality of the constant (unity), sine, and cosine functions in Eqs. (33–35), respectively,

$$\theta_1 = \theta_2 \tag{37}$$

That is, with uniform cross sections and identical umbilical attachment angles,

$$\left.\begin{aligned} L_1 &= L_2 \\ y_{c1} &= y_{c2} \\ z_{c1} &= z_{c2} \end{aligned}\right\} \Rightarrow \theta_1 = \theta_2 \tag{38}$$

It can be shown by simple substitution that the "only if" statement of Eq. (38) is, in fact, "if and only if" ($\Leftrightarrow$).

Using Eq. (36), one can expand Eq. (37) as follows:

$$\begin{aligned} \theta_1 &= \pm\sqrt{2\alpha_{11}(s_\xi - s_{\xi_c}) - 2\alpha_{21}(c_\xi - c_{\xi_c}) + (\alpha_{31}^2 + \alpha_{51})} \\ &= \pm\sqrt{2\alpha_{12}(s_\xi - s_{\xi_c}) - 2\alpha_{22}(c_\xi - c_{\xi_c}) + (\alpha_{32}^2 + \alpha_{52})} = \theta_2 \end{aligned} \tag{39}$$

Squaring and applying orthogonality as before, one concludes that

$$\theta_1 = \theta_2 \Rightarrow \begin{cases} \alpha_{11} = \alpha_{12} \\ \alpha_{21} = \alpha_{22} \\ \alpha_{31}^2 - \alpha_{51} = \alpha_{32}^2 - \alpha_{52} \end{cases} \tag{40}$$

Again, it can be shown by simple substitution that this relationship is actually if and only if.

In summary,

$$\left.\begin{aligned} L_1 &= L_2 \\ y_{c1} &= y_{c2} \\ z_{c1} &= z_{c2} \end{aligned}\right\} \Leftrightarrow \theta_1 = \theta_2 \Leftrightarrow \begin{cases} \alpha_{11} = \alpha_{12} \\ \alpha_{21} = \alpha_{22} \\ \alpha_{31}^2 - \alpha_{51} = \alpha_{32}^2 - \alpha_{52} \end{cases} \tag{41}$$

If the umbilicals also have identical initial curvatures, that is, for

$$\kappa_1^i(s) = \kappa_2^i(s) \quad \forall\ 0 \le s \le L \tag{42}$$

one has that

$$\alpha_{51}(s) = \alpha_{52}(s) \tag{43}$$

such that

$$\left.\begin{aligned} L_1 &= L_2 \\ y_{c1} &= y_{c2} \\ z_{c1} &= z_{c2} \end{aligned}\right\} \Leftrightarrow \theta_1 = \theta_2 \Leftrightarrow \begin{cases} \alpha_{11} = \alpha_{12} \\ \alpha_{21} = \alpha_{22} \\ \alpha_{31} = \pm\alpha_{32} \end{cases} \tag{44}$$

Equation (44) can be strengthened further as follows.

From Eq. (8),

$$\alpha_3 = \left.\frac{\mathrm{d}\xi}{\mathrm{d}s}\right|_{R\to C} \tag{45}$$

Also, from Eqs. (10) and (15),

$$\theta_1 = \theta_2 \Leftrightarrow \left(\frac{\mathrm{d}\xi}{\mathrm{d}s}\right)_1 = \left(\frac{\mathrm{d}\xi}{\mathrm{d}s}\right)_2 \quad \forall\ 0 \le s \le L \tag{46}$$

Therefore, for $\theta_1 = \theta_2$, one can conclude that

$$\alpha_{31} = \pm\alpha_{32} \Leftrightarrow \alpha_{31} = \alpha_{32} \tag{47}$$

In conclusion, if the two umbilicals have identical initial curvatures, Eq. (41) reduces to the following:

$$\left.\begin{aligned} L_1 &= L_2 \\ y_{c1} &= y_{c2} \\ z_{c1} &= z_{c2} \end{aligned}\right\} \Leftrightarrow \theta_1 = \theta_2 \Leftrightarrow \begin{cases} \alpha_{11} = \alpha_{12} \\ \alpha_{21} = \alpha_{22} \\ \alpha_{31} = \alpha_{32} \end{cases} \tag{48}$$

Equations (46) and (48) have the following physical significance: for a slender, terminally loaded umbilical (assuming only in-plane loading), a reference (relaxed) spatial configuration for which the curvature varies quadratically with arc length, and a specified terminal geometry, changing the flexural rigidity by an arbitrary factor γ changes all terminal loads by the same factor without changing the umbilical shape. The implications for in-plane umbilical flexibilities will be explored in the next section.

Flexibility Equations

For a given terminal geometry (ξ_c, y_c, and z_c), one can now differentiate Eqs. (17), (20), and (22) with respect to the three terminal loads to yield expressions for the nine in-plane translational flexibilities. For convenience, define the following "flexibility integrals":

$$\beta_1 = \int_{\xi_c}^{2\pi} \theta^{-3}\, \mathrm{d}\xi \tag{49}$$

$$\beta_2 = \int_{\xi_c}^{2\pi} \theta^{-3} c_\xi\, \mathrm{d}\xi \tag{50}$$

$$\beta_3 = \int_{\xi_c}^{2\pi} \theta^{-3} s_\xi \, \mathrm{d}\xi \tag{51}$$

$$\beta_4 = \int_{\xi_c}^{2\pi} \theta^{-3} c_\xi^2 \, \mathrm{d}\xi \tag{52}$$

$$\beta_5 = \int_{\xi_c}^{2\pi} \theta^{-3} c_\xi s_\xi \, \mathrm{d}\xi \tag{53}$$

and

$$\beta_6 = \int_{\xi_c}^{2\pi} \theta^{-3} s_\xi^2 \, \mathrm{d}\xi \tag{54}$$

where, from Eqs. (11) and (15),

$$\theta = \pm\sqrt{2\alpha_1(s_\xi - s_{\xi_c}) - 2\alpha_2(c_\xi - c_{\xi_c}) + \alpha_3^2} \tag{55}$$

According to Leibnitz's rule,

$$\frac{\partial}{\partial x}\int_{f(x)}^{g(x)} F(x,\xi)\,\mathrm{d}\xi = \int_{f(x)}^{g(x)} \frac{\partial}{\partial x} F(x,\xi)\,\mathrm{d}\xi + F[x,g(x)]\frac{\partial g(x)}{\partial x} - F[x,f(x)]\frac{\partial f(x)}{\partial x} \tag{56}$$

Applying Eq. (56) to Eq. (17), and substituting from Eqs. (23–27) and (49–54), one obtains the following expressions for the rotational flexibilities:

$$\frac{\partial \xi_c}{\partial Q_y} = \frac{\mp|\alpha_3|}{EI}\left[\frac{\beta_3 - s_{\xi_c}\beta_1}{1 \mp |\alpha_3|\alpha_4\beta_1}\right] \tag{57}$$

$$\frac{\partial \xi_c}{\partial Q_z} = \frac{\pm|\alpha_3|}{EI}\left[\frac{\beta_2 - c_{\xi_c}\beta_1}{1 \mp |\alpha_3|\alpha_4\beta_1}\right] \tag{58}$$

and

$$\frac{\partial \xi_c}{\partial M_x} = \frac{\mp|\alpha_3|\alpha_3}{EI}\left[\frac{\beta_1}{1 \mp |\alpha_3|\alpha_4\beta_1}\right] \tag{59}$$

Applying Leibnitz's rule now to Eqs. (20) and (22), and substituting from Eqs. (57–59), one obtains the remaining six (translational) flexibility equations. The translational flexibilities are as follows:

$$\frac{\partial y_c}{\partial Q_y} = \frac{-1}{EI}\left[(\beta_6 - s_{\xi_c}\beta_3) - (\beta_3 - s_{\xi_c}\beta_1)\left(\frac{s_{\xi_c} \mp |\alpha_3|\alpha_4\beta_3}{1 \mp |\alpha_3|\alpha_4\beta_1}\right)\right] \tag{60}$$

$$\frac{\partial y_c}{\partial Q_z} = \frac{1}{EI}\left[(\beta_5 - c_{\xi_c}\beta_3) - (\beta_2 - c_{\xi_c}\beta_1)\left(\frac{s_{\xi_c} \mp |\alpha_3|\alpha_4\beta_3}{1 \mp |\alpha_3|\alpha_4\beta_1}\right)\right] \tag{61}$$

$$\frac{\partial y_c}{\partial M_x} = \frac{-\alpha_3}{EI}\left[\beta_3 - \beta_1\left(\frac{s_{\xi_c} \mp |\alpha_3|\alpha_4\beta_3}{1 \mp |\alpha_3|\alpha_4\beta_1}\right)\right] \tag{62}$$

$$\frac{\partial z_c}{\partial Q_y} = \frac{1}{EI}\left[(\beta_5 - s_{\xi_c}\beta_2) - (\beta_3 - s_{\xi_c}\beta_1)\left(\frac{c_{\xi_c} \mp |\alpha_3|\alpha_4\beta_2}{1 \mp |\alpha_3|\alpha_4\beta_1}\right)\right] \tag{63}$$

$$\frac{\partial z_c}{\partial Q_z} = \frac{-1}{EI}\left[(\beta_4 - c_{\xi_c}\beta_2) - (\beta_2 - c_{\xi_c}\beta_1)\left(\frac{c_{\xi_c} \mp |\alpha_3|\alpha_4\beta_2}{1 \mp |\alpha_3|\alpha_4\beta_1}\right)\right] \tag{64}$$

and

$$\frac{\partial z_c}{\partial M_x} = \frac{\alpha_3}{EI}\left[\beta_2 - \beta_1\left(\frac{c_{\xi_c} \mp |\alpha_3|\alpha_4\beta_2}{1 \mp |\alpha_3|\alpha_4\beta_1}\right)\right] \tag{65}$$

An example derivation of a translational flexibility is provided in the Appendix.

End-State Verification

To verify the expressions for end-state geometry [i.e., Eqs. (17), (20), and (22)], a set of combined end loads Q_y, Q_z, and M_x was initially selected, for an example umbilical, with the results to be compared with those of a corresponding finite element simulation. The loads were then varied proportionally by use of a load-magnification factor λ to produce a family of loading conditions for comparison purposes. The finite element model was built using the commercially available package COSMOS/DesignStar using thin-shell triangular elements with a subsequent solution obtained via the supplied nonlinear solver. The thin-shell element present in COSMOS/DesignStar is formulated using Kirchhoff assumptions (i.e., neglecting transverse-shear deformations) analogous to the underlying assumptions of the present beam formulation. The use of thin-shell shell elements to construct the comparative finite element model is therefore kinematically appropriate.

The example umbilical has a rectangular cross section and forms a quarter circle of radius ρ in its relaxed configuration, with assigned values for ρ, for length L, and for flexural rigidity EI. The finite element model comprises 40 equally sized triangular shell elements composed of a linearly elastic material of assigned Young's modulus E, and Poisson's ratio ν. In particular, the selected umbilical parameters are $\rho = 63.662$ mm, $L = 100$ mm, $EI = 1250\ \mathrm{N \cdot mm^2}$, $E = 7.5 \cdot 10^{12}\ \mathrm{N/m^2}$, and $\nu = 0.28$. Its cross-sectional width is 2 mm, and its height (i.e., shell thickness) is 0.1 mm. The assigned end loads are $Q_y = 0.01\lambda$ N, $Q_z = -0.01\lambda$ N, and $M_x = -25\lambda\ \mathrm{N \cdot mm}$, where λ varies from 0.01 to 1.0, in increments of 0.01.

Calculations were made of the terminal geometry (y_c, z_c, ξ_c) from the analytical expressions [Eqs. (17), (20), and (22)], for each value of λ, using an iterative process in which an initial guess was made for the end angle ξ_c, followed by formation of the shape kernel θ [Eqs. (11) and (15)], and by calculation of the resulting length L [using a numerical approximation of Eq. (17)]. Based on the error in L, a new estimate for ξ_c was determined by adding an amount proportional to the calculated error. The iterations were continued until the percent error calculated for L was less than $1.0 \cdot 10^{-7}$. After convergence, the end coordinates (y_c, z_c) were calculated using Eqs. (20) and (22). The resulting terminal geometry is presented in Fig. 2a, as a function of λ, by solid lines.

The finite element model was then used to verify the previously calculated terminal geometry by determining the end coordinates (y_c, z_c) for the various values of λ. The results are shown as markers in Fig. 2a. The results from the analytical model (solid lines) and those from the finite element model were found to be in excellent agreement. Figure 3 shows the initial and final configurations of the example umbilical for $\lambda = 1$.

Flexibility Verification

Once the end-states had been verified, they could be used in turn to verify the flexibility equations [Eqs. (57–65)], by finite difference approximations calculated over the selected range of values for λ. The value chosen for each of the increments ΔQ_y, ΔQ_z, and ΔM_x corresponds to a 0.01% change from the respective nominal value. Finite difference results for the flexibilities are shown as markers in Figs. 2b–2d. The analytical models (shown by solid lines) are seen to be in excellent agreement with the finite difference calculations.

Implications for Umbilical Design

The foregoing equations can be used as an aid for designing umbilicals to minimize static stiffness. First, the flexural rigidity can

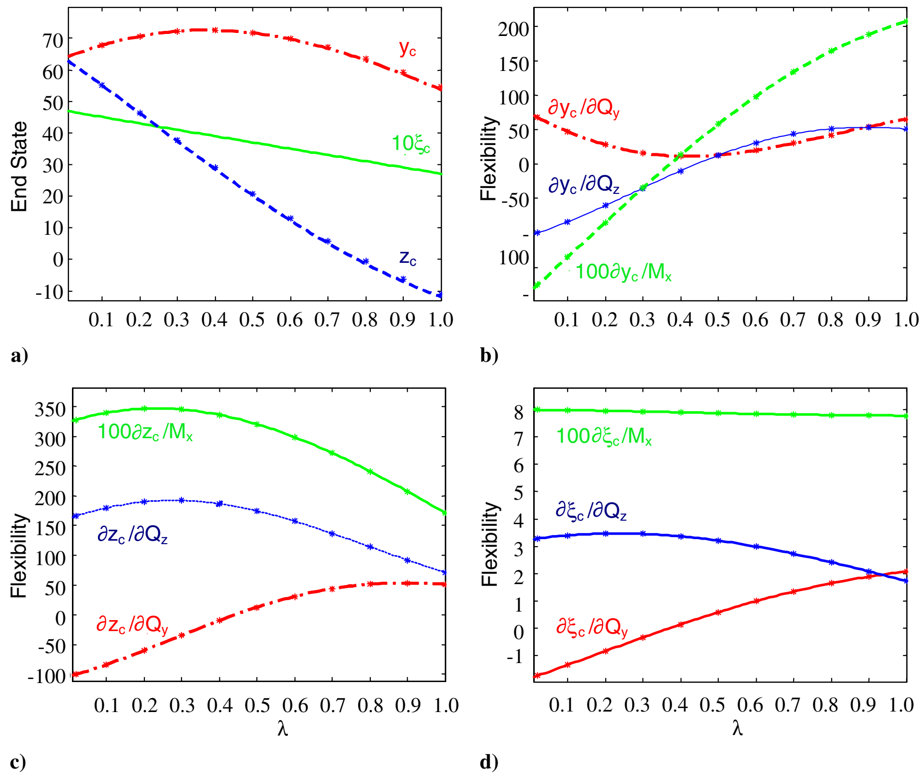

Fig. 2 End state and flexibilities vs load factor λ, for curved (quarter circle) umbilicals with flexural rigidity $EI = 1250\ \mathrm{N \cdot mm^2}$, length $L = 100$ mm, radius of curvature $\rho = 63.662$ mm (curvature $\kappa^i = -0.01571\ \mathrm{mm^{-1}}$), and end loadings $Q_y = 0.01\lambda$ N, $Q_z = -0.01\lambda$ N, and $M_x = -25\lambda\ \mathrm{N \cdot mm}$, where λ varies from 0.01 to 1.0 in increments of 0.01. Solid lines denote results calculated using the analytical expressions, markers denote results calculated using either a) the finite element model, or b-d) finite difference approximations.

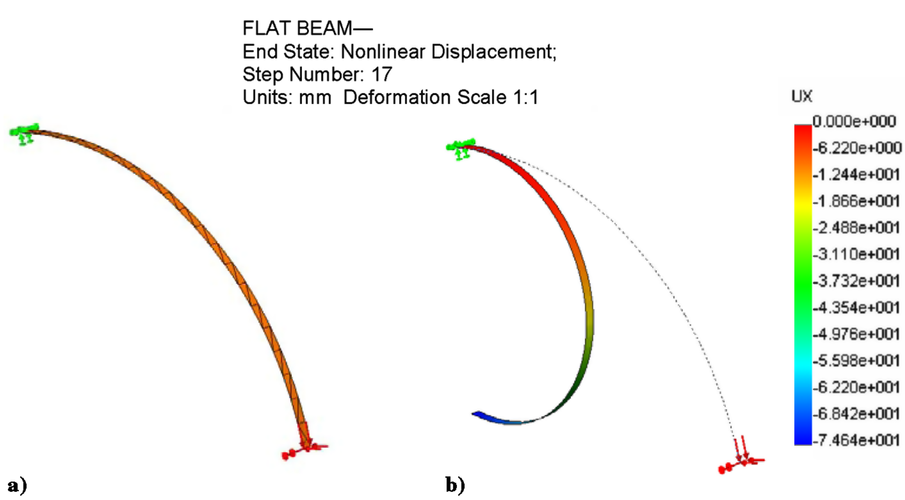

Fig. 3 Finite element model of the example umbilical defined in the caption of Fig. 2. The physical umbilical modeled has a rectangular cross section of width 2 mm and height (i.e., shell thickness) of 0.1 mm. The finite element discretization comprises 40 equally sized triangular shell elements composed of a linearly elastic material, defined by Young's modulus $E = 7.5\mathrm{E} + 12\ \mathrm{N/m^2}$ and Poisson's ratio $\nu = 0.28$. The resulting EI of the model equals $1250\ \mathrm{N \cdot mm^2}$, as required. Shown is the model in its a) undeformed state, and b) deformed state, after a loading corresponding to $\lambda = 1.0$. The analysis was carried out using the nonlinear solver incorporated into the commercial package COSMOS/DesignStar.

be used to adjust all stiffnesses by a common factor. Because all of the α_is and β_is are invariant with flexural rigidity, the square-bracketed factors of the flexibility equations, Eqs. (57–65), are all independent of flexural rigidity. It is evident from these equations, then, that reductions in EI will produce proportional reductions in all terminal loads and in-plane stiffnesses. Second, for given umbilical length L, and endpoint conditions ξ_c, Q_y, and Q_z, Eqs. (17), (20), and (22) can be solved for the loads Q_y, Q_z, and M_x. These loads can be determined and used iteratively in the flexibility equations to optimize the umbilical flexibilities (or, equivalently, the corresponding stiffnesses) using L as a parameter. Third, the umbilical designer can use these equations to determine optimal L, ξ_c combinations. Although the angle ξ_c is fixed at about 225 deg for ARIS (in the home, or centered, position), L and ξ_c optimization could suggest better angles for future designs. After obtaining a satisfactory design for the static stiffnesses, the designer could determine the umbilical's dynamic response via simulations using, for example, the geometrically exact beam formulation [17–20,23].

Conclusions

This research has presented equations for the shape and flexibilities of a slender umbilical on orbit (that is, such that gravity can be neglected), under general, terminal, in-plane loading conditions of sufficient magnitude to cause large deformations. The relaxed (preloaded) umbilical was assumed to have a curvature following a quadratic function of arc length and to have a uniform cross section. The loaded umbilical was assumed to undergo no plastic deformation. All in-plane stiffnesses were shown to be proportional to the flexural rigidity EI. The geometric end state and umbilical flexibility equations were verified numerically for an initially circular umbilical, subject to in-plane end-loading conditions. An approach was offered for using umbilical length and terminal geometry (endpoint locations and slopes) to optimize these umbilical stiffnesses.

Appendix: Sample Derivation of a Flexibility Equation

From Eq. (20), the y coordinate of terminal point C is [20]

$$y_c = \int_{\xi_c}^{2\pi} \theta^{-1} s_\xi \, \mathrm{d}\xi \tag{A1}$$

where [37]

$$\theta(\xi) = \pm[2\alpha_1(s_\xi - s_{\xi_c}) - 2\alpha_2(c_\xi - c_{\xi_c}) + (\alpha_3^2 + \alpha_5)]^{1/2} \tag{A2}$$

for [23–25]

$$\alpha_1 = \frac{Q_y}{EI} \tag{A3}$$

$$\alpha_2 = \frac{Q_z}{EI} \tag{A4}$$

$$\alpha_3 = \frac{M_x}{EI} + \kappa_c^i \tag{A5}$$

and [27]

$$\alpha_5 = (\kappa^i)^2 - (\kappa_c^i)^2 \tag{A6}$$

Taking the partial derivative of Eq. (A1) with respect to Q_y, one has

$$\frac{\partial y_c}{\partial Q_y} = \frac{\partial}{\partial Q_y}\left(\int_{\xi_c}^{2\pi} \theta^{-1} s_\xi \, \mathrm{d}\xi\right) \tag{A7}$$

Applying Leibnitz's rule,

$$\frac{\partial y_c}{\partial Q_y} = \int_{\xi_c}^{2\pi} \frac{\partial}{\partial Q_y}(\theta^{-1} s_\xi)\, \mathrm{d}\xi + (\theta^{-1} s_\xi)|_{\xi\to 2\pi} \frac{\partial(2\pi)}{\partial Q_y} - (\theta^{-1} s_\xi)|_{\xi\to\xi_c} \frac{\partial \xi_c}{\partial Q_y} \tag{A8}$$

The right-hand side of this equation will next be evaluated term by term.

The integrand of the first right-hand side term is

$$\frac{\partial}{\partial Q_y}(\theta^{-1} s_\xi) = -s_\xi \theta^{-3}\left[\frac{1}{EI}(s_\xi - s_{\xi_c}) - (\alpha_1 c_{\xi_c} + \alpha_2 s_{\xi_c})\frac{\partial \xi_c}{\partial Q_y}\right] \tag{A9}$$

so that the integral itself becomes

$$\int_{\xi_c}^{2\pi} \frac{\partial}{\partial Q_y}(\theta^{-1} s_\xi)\, \mathrm{d}\xi = \frac{-1}{EI}\left(\int_{\xi_c}^{2\pi} s_\xi^2 \theta^{-3}\, \mathrm{d}\xi - s_{\xi_c}\int_{\xi_c}^{2\pi} s_\xi \theta^{-3}\, \mathrm{d}\xi\right) + (\alpha_1 c_{\xi_c} + \alpha_2 s_{\xi_c})\int_{\xi_c}^{2\pi} s_\xi \theta^{-3}\, \mathrm{d}\xi \frac{\partial \xi_c}{\partial Q_y} \tag{A10}$$

The second right-hand side term of Eq. (A8) is zero, since 2π is a constant.

The third right-hand side term is

$$-(\theta^{-1} s_\xi)|_{\xi\to\xi_c} \frac{\partial \xi_c}{\partial Q_y} = -(\pm|\alpha_3|^{-1} s_{\xi_c})\frac{\partial \xi_c}{\partial Q_y} \tag{A11}$$

where the sign accompanying $|\alpha_3|^{-1}$ is that of slope $\mathrm{d}\xi/\mathrm{d}s$. By similar application of Leibnitz's rule to the equation [17]

$$L = -\int_{\xi_c}^{2\pi} \theta^{-1}\, \mathrm{d}\xi \tag{A12}$$

one has

$$\frac{\partial \xi_c}{\partial Q_y} = \frac{\mp|\alpha_3|}{EI}\left[\frac{\int_{\xi_c}^{2\pi} \theta^{-3} s_\xi\, \mathrm{d}\xi - s_{\xi_c}\int_{\xi_c}^{2\pi} \theta^{-3}\, \mathrm{d}\xi}{1 \mp |\alpha_3|\alpha_4 \int_{\xi_c}^{2\pi} \theta^{-3}\, \mathrm{d}\xi}\right] \tag{A13}$$

Substituting from Eqs. (A9), (A11), and (A13) into Eq. (A8), and using Eqs. (49), (51), and (54) to reexpress the result in terms of the β_is, one obtains the form given in Eq. (60):

$$\frac{\partial y_c}{\partial Q_y} = \frac{-1}{EI}\left[(\beta_6 - s_{\xi_c}\beta_3) - (\beta_3 - s_{\xi_c}\beta_1)\left(\frac{s_{\xi_c} \mp |\alpha_3|\alpha_4\beta_3}{1 \mp |\alpha_3|\alpha_4\beta_1}\right)\right] \tag{A14}$$

The other flexibility equations can be determined analogously.

References

[1] Edberg, D. L., and Wilson, B. W., "Design and Testing of Reduced-Stiffness Umbilicals for Space Station Microgravity Isolation," AIAA Paper 2000-1408, April 2000.

[2] Hummel, F. H., and Morton, W. B., "On the Large Deflection of Thin Flexible Strips and the Measurement of Their Elasticity," *Philosophical Magazine*, Series 7, Vol. 17, 1927, pp. 348–357.

[3] Gross, S., and Lehr, E., *Die Federn*, V. D. I. Verlag, Berlin, Germany, 1938.

[4] Barten, H. J., "On the Deflection of a Cantilever Beam," *Quarterly of Applied Mathematics*, Vol. 2, No. 2, 1944, pp. 168–171.

[5] Barten, H. J., "On the Deflection of a Cantilever Beam," *Quarterly of Applied Mathematics*, Vol. 3, No. 3, 1945, pp. 275–276.

[6] Bisshopp, K. E., and Drucker, D. C., "Large Deflections of Cantilever Beams," *Quarterly of Applied Mathematics*, Vol. 3, No. 3, Oct. 1945, pp. 272–275.

[7] Bickley, W. G., "The Heavy Elastica," *Philosophical Magazine*, Series 7, Vol. 17, 1934, pp. 603–622.

[8] Rohde, F. V., "Large Deflections of a Cantilever Beam with a Uniformly Distributed Load," *Quarterly of Applied Mathematics*, Vol. 11, No. 3, 1953, pp. 337–338.

[9] Schmidt, R., and Dadeppo, D. A., "Large Deflections of Heavy Cantilever Beams and Columns," *Quarterly of Applied Mathematics*, Vol. 28, Oct. 1970, pp. 441–444.

[10] Mitchell, T. P., "The Non-Linear Bending of Thin Rods," *Journal of Applied Mechanics*, Vol. 26, March 1959, pp. 40–43.

[11] Beth, R. A., and Wells, C. P., "Finite Deflections of a Cantilever Strut," *Journal of Applied Physics*, Vol. 22, No. 6, 1951, pp. 742–746. doi:10.1063/1.1700042

[12] Massoud, M. F., "On the Problem of Large Deflection of a Cantilever Beam," *International Journal of Mechanical Sciences*, Vol. 8, Feb. 1966, pp. 141–143. doi:10.1016/0020-7403(66)90072-5

[13] Frisch-Fay, R., *Flexible Bars*, Butterworths, London, 1962, pp. 5, 42.

[14] Antman, S. S., Marlow, R. S., and Vlahacos, C. P., "The Complicated Dynamics of Heavy Rigid Bodies Attached to Deformable Rods," *Quarterly of Applied Mathematics*, Vol. 56, No. 3, Sept. 1998, pp. 431–460.

[15] Chucheepsakul, S., Buncharoen, S., and Huang, T., "Elastica of Simple Variable-Arc-Length Beam Subjected to End Moment," *Journal of Engineering Mechanics*, Vol. 121, No. 7, July 1995, pp. 767–772. doi:10.1061/(ASCE)0733-9399(1995)121:7(767)

[16] Manuel, F. S., and Lee, S. L., "Flexible Bars Subjected to Arbitrary Discrete Loads and Boundary Conditions," *Journal of the Franklin Institute*, Vol. 285, No. 6, 1968, pp. 452–474. doi:10.1016/0016-0032(68)90050-1

[17] Vu-Quoc, L., "Dynamics of Flexible Structures Performing Large Overall Motions: A Geometrically Nonlinear Approach," Ph.D. Dissertation, ERL Memorandum UCB/ERL M86/36, Univ. of California, Berkeley, CA, May 1986.

[18] Simo, J. C., and Vu-Quoc, L., "On the Dynamics of Flexible Beams Under Large Overall Motions, The Plane Case: Part 1," *Journal of Applied Mechanics*, Vol. 53, Dec. 1986, pp. 849–854.

[19] Simo, J. C., and Vu-Quoc, L., "On the Dynamics of Flexible Beams Under Large Overall Motions, The Plane Case: Part 2," *Journal of Applied Mechanics*, Vol. 53, Dec. 1986, pp. 855–863.

[20] Simo, J. C., and Vu-Quoc, L., "Three-Dimensional Finite Strain Rod Model, Part 2: Computational Aspects," *Computer Methods in Applied Mechanics and Engineering*, Vol. 58, No. 1, 1986, pp. 79–116. doi:10.1016/0045-7825(86)90079-4

[21] Simo, J. C., and Vu-Quoc, L., "The Role of Nonlinear Theories in Transient Dynamics Analysis of Flexible Structures," *Journal of Sound and Vibration*, Vol. 119, No. 3, 1987, pp. 487–508. doi:10.1016/0022-460X(87)90410-X

[22] Vu-Quoc, L., and Simo, J. C., "On the Dynamics of Earth-Orbiting Flexible Satellites with Multibody Components," *Journal of Guidance, Control, and Dynamics*, Vol. 10, No. 6, Nov.–Dec. 1987, pp. 549–558, Paper G87-088.

[23] Simo, J. C., and Vu-Quoc, L., "On the Dynamics in Space of Rods Undergoing Large Motions: A Geometrically Exact Approach," *Computer Methods in Applied Mechanics and Engineering*, Vol. 66, No. 2, 1988, pp. 125–161. doi:10.1016/0045-7825(88)90073-4

[24] Crespo da Silva, M. R. M., "Non-Linear Flexural-Torsional-Extensional Dynamics of Beams, 1: Formulation," *International Journal of Solids and Structures*, Vol. 24, No. 12, 1988, pp. 1225–1234. doi:10.1016/0020-7683(88)90087-X

[25] Simo, J. C., and Vu-Quoc, L., "A Geometrically Exact Rod Model Incorporating Shear and Torsion Warping Deformation," *International Journal of Solids and Structures*, Vol. 27, No. 3, 1991, pp. 371–393. doi:10.1016/0020-7683(91)90089-X

[26] McRobie, F. A., and Lasenby, J., "Simo-Vu Quoc Rods Using Clifford Algebra," *International Journal for Numerical Methods in Engineering*, Vol. 45, No. 4, 1999, pp. 377–398. doi:10.1002/(SICI)1097-0207(19990610)45:4<377::AID-NME586>3.0.CO;2-P

[27] Rojahn, C., "Large Deflections of Elastic Beams," Degree of Engineer Thesis, Stanford Univ., Palo Alto, CA, June 1968.

[28] Gorski, W., "A Review of the Literature and a Bibliography on Finite Elastic Deflections of Bars," *Institute of Engineers, Australia: Civil Engineering Transactions*, Vol. CE18, No. 2, 1976, pp. 74–85.

[29] Libai, A., and Simmonds, J. G., *The Nonlinear Theory of Elastic Shells*, 2nd ed., Cambridge Univ. Press, Cambridge, England, U. K., 1998.

[30] Ibrahimbegovic, A., Frey, F., and Kozar, I., "Computational Aspects of Vector-Like Parametrization of Three-Dimensional Finite Rotations," *International Journal for Numerical Methods in Engineering*, Vol. 38, No. 21, 1995, pp. 3653–3673. doi:10.1002/nme.1620382107

[31] Ibrahimbegovic, A., "On Finite Element Implementation of Geometrically Nonlinear Reissner's Beam Theory: Three-Dimensional Curved Beam Elements," *Computer Methods in Applied Mechanics and Engineering*, Vol. 122, No. 1, 1995, pp. 11–26. doi:10.1016/0045-7825(95)00724-F

[32] Iura, M., and Atluri, S. N., "Dynamic Analysis of Finitely Stretched and Rotated Three-Dimensional Space-Curved Beams," *Computers and Structures*, Vol. 29, No. 5, 1988, pp. 875–889. doi:10.1016/0045-7949(88)90355-0

[33] Kapania, R. K., and Li, J., "A Formulation and Implementation of Geometrically Exact Curved Beam Elements Incorporating Finite Strains and Finite Rotations," *Computational Mechanics*, Vol. 30, Nos. 5–6, April 2003, pp. 444–459. doi:10.1007/s00466-003-0422-7

[34] Kapania, R. K., and Li, J., "On a Geometrically Exact Curved/Twisted Beam Theory Under Rigid Cross Section Assumption," *Computational Mechanics*, Vol. 30, Nos. 5–6, April 2003, pp. 428–443. doi:10.1007/s00466-003-0421-8

[35] Hodges, D. H., "Geometrically Exact, Intrinsic Theory for Dynamics of Curved and Twisted Anisotropic Beams," *AIAA Journal*, Vol. 41, No. 6, 2003, pp. 1131–1137.

[36] Iura, M., and Atluri, S. N., "On a Consistent Theory, and Variational Formulation of Finitely Stretched and Rotated 3-D Space-Curved Beams," *Computational Mechanics*, Vol. 4, No. 2, March 1988, pp. 73–88. doi:10.1007/BF00282411

[37] Hampton, R. D., Quraishi, N., and Rupert, J. K., "Flexibility Equations for Active Rack Isolation System Umbilicals with Planar End Loading (TN)," *AIAA Journal*, Vol. 39, No. 10, Oct. 2001, pp. 2024–2027.

R. Kapania
Associate Editor